

Discussions on the Line-shape of $X(4660)$ Resonance

QIN-FANG CAO¹, HONG-RONG QI², YU-FEI WANG¹, HAN-QING ZHENG^{1,3}

¹*Department of Physics and State Key Laboratory of Nuclear Physics and Technology, Peking University, Beijing 100871, China*

²*School of Physics, Beihang University, Beijing 100191, China*

³*Collaborative Innovation Center of Quantum Matter, Beijing 100871, China*

May 4, 2022

Abstract

A careful re-analysis is made on $e^+e^- \rightarrow X(4660) \rightarrow (\Lambda_c\bar{\Lambda}_c)/(\psi'\pi\pi)$ processes, aiming at resolving the apparent conflicts between Belle and BESIII data above $\Lambda_c\bar{\Lambda}_c$ threshold. We use a model containing a Breit-Wigner resonance and $\Lambda_c\bar{\Lambda}_c$ four-point contact interactions, with which the enhancement right above $\Lambda_c\bar{\Lambda}_c$ threshold is well explained by a virtual pole generated by $\Lambda_c\bar{\Lambda}_c$ attractive final state interaction, located at $M_V = 4.566 \pm 0.007$ GeV. Meanwhile, $X(4660)$ remains to be a typical Breit-Wigner resonance, and is hence of confinement nature. Our analysis strongly suggests the existence of the virtual pole with statistical significance of 4.2 standard deviation (σ). Nevertheless, the conclusion crucially depends on the line-shape of cross sections which are of limited statistics, hence we urge new experimental analyses from Belle II, BESIII, and LHCb to settle down the issue.

Since the discovery of $X(3872)$ in 2003 [1], hadronic exotic states, or called “ XYZ ” states, open a new window for hadron physics researches. Those states do not match the energy level positions predicted by naive quark models (e.g. the the Godfrey-Isgur model in $c\bar{c}$ sector [2]), and most of them are very narrow despite of locating above open charm (bottom) thresholds, which have intrigued theorists for recent years. Various models are established to understand such states: for example, modified quark models [3–5] which treat them as confining states; “non-resonance” interpretations regarding them as branch cut singularities [6]; also, one widely accepted mechanism is so called “hadronic molecules” [7–10].

Particularly, in 2007, Belle collaboration observed two structures, dubbed as $X(4630)$ and $X(4660)$, in cross-section shape of $e^+e^- \rightarrow \gamma_{ISR}\psi'\pi^+\pi^-$ with quantum number $J^{PC} = 1^{--}$ [11]. This discovery is confirmed later by Babar collaboration [12] and updated observation of Belle [13]. Moreover, the investigation of $e^+e^- \rightarrow \gamma_{ISR}\Lambda_c\bar{\Lambda}_c$ process by Belle collaboration reveals an “exotic” state called $X(4630)$ [14]. It is believed that $X(4630)$ and $X(4660)$ may in fact be the same state [15–17], and various interpretations are proposed, see e.g. Refs. [17–22].

More recently, a much precise measurement by BESIII collaboration gives the cross sections at four center-of-mass energies for $e^+e^- \rightarrow \Lambda_c\bar{\Lambda}_c$ cross section near $\Lambda_c\bar{\Lambda}_c$ threshold [23]. As shown in Fig. 2 of Ref. [23] (or the left panel of Fig. 3 in this paper), the BESIII data is questioned to have conflicts with the Belle data [15, 24]: especially the line-shape of BESIII data appears nearly horizontal while that from Belle shows a significant growth. The results from some earlier works are not compatible with BESIII data, see e.g. Fig. 2 of Ref. [17].

This work aims at disentangling this problem: it is suggested that a virtual pole via $\Lambda_c\bar{\Lambda}_c$ contact interactions, in addition to the $X(4660)$ Breit-Wigner resonance, could well explain the odd line-shape which are failed to be described by previous studies.

¹In this paper ψ' denotes the $\psi(2S)$ particle.

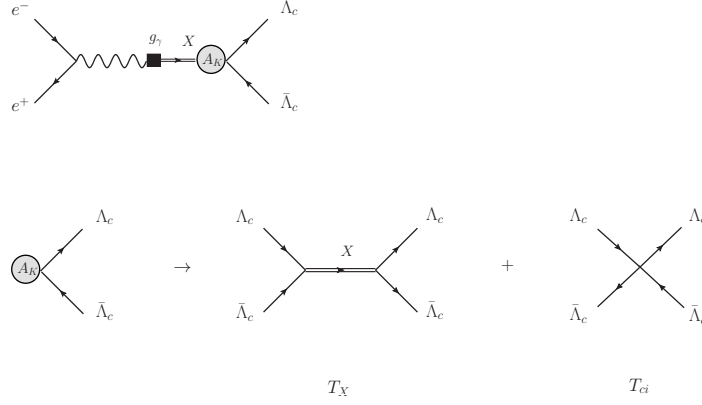


Figure 1: The Feynman diagram of $e^+e^- \rightarrow X(4660) \rightarrow \Lambda_c \bar{\Lambda}_c$. A_K is the K matrix sector in Eq. (4).

To begin with, we assume that $X(4630)$ and $X(4660)$ are the same particle and denote it as X , with quantum number $^{2s+1}L_J = ^3S_1$ ². For $\Lambda_c \bar{\Lambda}_c$ channel, the coupling among $X\Lambda_c \bar{\Lambda}_c$ and the QED transition from a photon to X are introduced as following:

$$\mathcal{L}_{X\Lambda_c} = g_1 \bar{\Lambda}_c \gamma^\mu X_\mu \Lambda_c, \quad \mathcal{L}_{\gamma X} = g_\gamma X^{\mu\nu} F_{\nu\mu}; \quad (1)$$

where $X^{\mu\nu}$ and $F_{\nu\mu}$ are the strength tensors of the X and the photon, respectively. The contact interaction between $\Lambda_c \bar{\Lambda}_c$ is

$$\mathcal{L}_{\Lambda_c \bar{\Lambda}_c} = C_V (\bar{\Lambda}_c \gamma_\mu \Lambda_c) (\bar{\Lambda}_c \gamma^\mu \Lambda_c) + C_A (\bar{\Lambda}_c \gamma_\mu \gamma^5 \Lambda_c) (\bar{\Lambda}_c \gamma^\mu \gamma^5 \Lambda_c), \quad (2)$$

which simulates vector and axial-vector meson exchanges³. For $\psi' \pi \pi$ channel, the interactions may be complicated with various Lorentz structures, but only the final two pions with total isospin and angular momentum $IJ = 00$ and their final state interaction (FSI) are considered, just like Ref. [26]. Therefore the momentum dependence from derivative couplings of pions can be absorbed into their FSI, leaving the effective vertices as following

$$V_f^{X\psi\pi} \propto g_2 \mathcal{A}_{\pi\pi}, \quad V_f^{\Lambda_c \psi\pi} \propto g_3 \mathcal{A}_{\pi\pi}, \quad (3)$$

where $g_{2,3}$ are fit parameters and the $\mathcal{A}_{\pi\pi}$ stands for the FSI term between two pions (see e.g. Ref. [26]).

Based on Eqs. (1), (2) and (3), a model of K matrix type concerning a mixed mechanism of s channel X state and $\Lambda_c \bar{\Lambda}_c$ contact interaction, can be established as shown in Figs. 1 and 2⁴. Specifically, the K matrix sector satisfying final state theorem is

$$A_K = \frac{1}{1 - i\rho K} = \frac{1}{1 - i\rho(T_X + T_{ci})}, \quad (4)$$

$$\rho = \sqrt{\frac{s - 4m^2}{s}},$$

where T_X and T_{ci} label the tree diagrams of s channel $\Lambda_c \bar{\Lambda}_c \rightarrow X(4660) \rightarrow \Lambda_c \bar{\Lambda}_c$, and $\Lambda_c \bar{\Lambda}_c$ contact vertex as FSI in 3S_1 channel, respectively, see Fig. 1; m is the mass of Λ_c . Note that

²The S - D mixing is omitted since it is suppressed in near-threshold region. For the standard method to calculate amplitudes in JLS basis, see e.g. Ref. [25].

³We have considered other types of contact terms, but they cannot fit the data well.

⁴The case with only FSI of $\Lambda_c \bar{\Lambda}_c$ is not considered in our model because it can not reproduce the $X(4660)$ peak in the fit. Moreover, the diagrams with $\gamma \rightarrow \Lambda_c \bar{\Lambda}_c$ vertices is considered as backgrounds since in those diagrams there are no bare $X(4660)$ propagators, causing a zero at $s = M_X^2$.

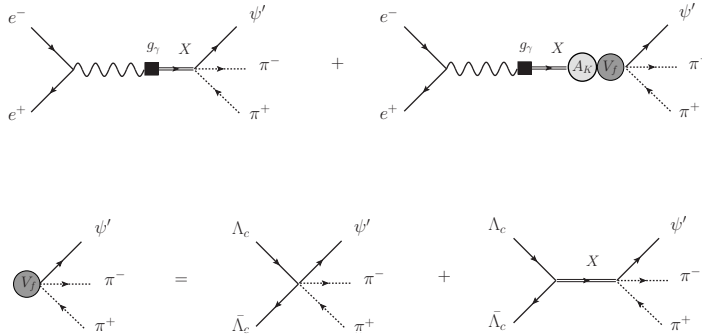


Figure 2: The Feynman diagram of $e^+e^- \rightarrow X(4660) \rightarrow \psi'\pi\pi$. A_K is the K matrix sector in Eq. (4) (the same as Fig. 1), and V_f is the vertex concerning $\psi'\pi\pi$ final state.

the $\psi'\pi\pi$ state does not show up in the above K matrix, instead it only appears as final state. This greatly simplifies the calculation since it reduces the couple channel problem to a single channel approximation. This simplification is justifiable, as discussed in Ref. [26], because the $\psi'\pi\pi$ threshold is distant from the energy region near $X(4660)$, giving a renormalization effect to Λ_c . More importantly, the smallness of g_2 in Eq. (3) is fully consistent with experimental observations (see Eq. (5)). Finally, in each channel we adopt a complex number serving as coherent background in the scattering amplitude.

Under the above formulations a combined fit to the data from both Belle [13, 14] and BESIII [23, 27] (also Babar data [12] for $\psi'\pi\pi$ final state) is performed, with a quite good fit quality $\chi^2/\text{d.o.f.} = 26.6/33$, indicating that the present model is compatible with both Belle and BESIII data. As shown in Fig. 3, it is evident that the good fit quality originates from an enhancement near the $\Lambda_c\bar{\Lambda}_c$ threshold. Further investigations find that a virtual state lying below but very close to $\Lambda_c\bar{\Lambda}_c$ threshold, located at $M_V = 4.566 \pm 0.007$ GeV, causes the enhancement. The main fit results are summarized in Table. 1.

| Parameters | Values |
|--------------------------|---------------------|
| M_{pole} (GeV) | 4.645 ± 0.028 |
| Γ_{pole} (GeV) | 0.078 ± 0.029 |
| M_V (GeV) | 4.566 ± 0.007 |
| M_X (GeV) | 4.604 ± 0.020 |
| g_1 | 2.151 ± 0.279 |
| λ (GeV $^{-2}$) | -15.899 ± 2.718 |

Table 1: Pole positions and fit parameters. M_{pole} and Γ_{pole} stands for the pole mass and width of $X(4660)$, respectively; M_V is the position of the virtual state. The other parameters are those related to the poles: M_X is the bare mass of $X(4660)$, g_1 is the coupling constant in Eq. (1), and $\lambda \equiv 3C_V + C_A$, see Eq. (2).

To proceed, the statistical significance of such virtual pole is studied. As a control, only Breit-Wigner effect is employed to fit all the data, giving the mass and width of $X(4660)$ as $M_{pole} = 4.674 \pm 0.043$ GeV and $\Gamma_{pole} = 0.147 \pm 0.110$ GeV, but the fit quality becomes $\chi^2/\text{d.o.f.} = 44.4/34$. Comparing with the mixture mechanism ($\chi^2/\text{d.o.f.} = 26.6/33$), the statistical significance of the virtual state is obtained to be 4.2σ , indicating strong evidence in support of the virtual pole as truly existing. Furthermore, to test the stability of the poles, we also use the Breit - Wigner term for $X(4360)$ to replace the constant coherent background, with the mass and width fixed, while the residue varies. Even though the behaviour near $\psi'\pi\pi$ threshold changes a little (see Fig. 4), the pole positions are found to be stable against the

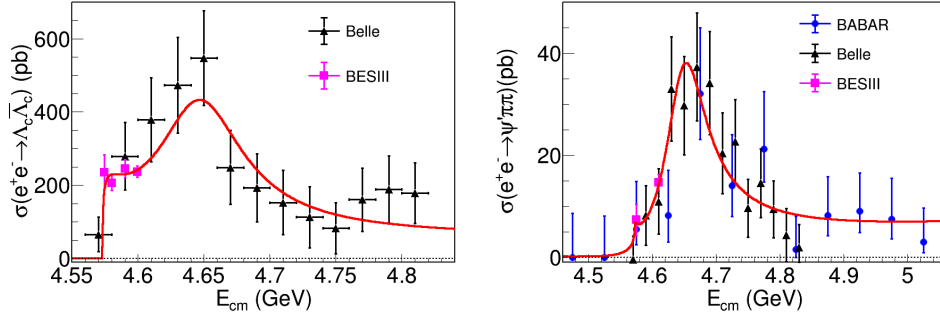


Figure 3: The fit (red solid curves) to data of relevant processes with constant coherent background.

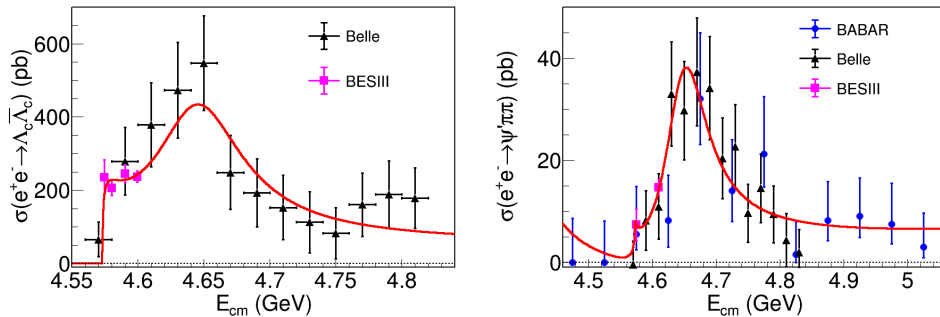


Figure 4: The fit (red solid curves) to data of relevant processes with explicit $X(4360)$ Breit - Wigner term.

variation of backgrounds: the virtual state locates at $M_V = 4.566 \pm 0.003$ GeV, and $X(4660)$ pole $M_{pole} = 4.643 \pm 0.011$ GeV and $\Gamma_{pole} = 0.080 \pm 0.019$ GeV.

It should be emphasized that from a general point of view in quantum scattering theories, virtual states are believed to arise in attractive interactions that are not strong enough, being “precursors” of bound states: when the attractive coupling is strong enough they become bound states. In Table. 1 the parameter λ indicates the attractive force between Λ_c and $\bar{\Lambda}_c$. Figure. 5 shows the trajectory of the poles against the increase of $|\lambda|$: when the $\Lambda_c \bar{\Lambda}_c$ contact interaction grows stronger, the virtual pole moves closer to the threshold; meanwhile, the $X(4660)$ resonance becomes narrower. It is worth noticing that the pole trajectory is model dependent: if the kinematic factor $i\rho$ were replaced by the entire two point function B_0 , the virtual pole would go up to the first sheet and become a bound state, given a large enough $|\lambda|$. All in all, these analyses exhibits a very clear physical picture: the virtual pole is produced by FSI, while $X(4660)$ state is a typical Breit-Wigner state with a pair of nearby poles. According to the pole counting rule [28] (which has been successfully applied to the studies of “XYZ” physics in Refs. [26, 29–31]), our analysis suggests that $X(4660)$ is of confinement nature.

Furthermore, the ratio between the decay widths $\Gamma(X \rightarrow \Lambda_c \bar{\Lambda}_c)$ and $\Gamma(X \rightarrow \psi' \pi \pi)$ can also be estimated as:

$$\frac{\Gamma(X \rightarrow \Lambda_c \bar{\Lambda}_c)}{\Gamma(X \rightarrow \psi' \pi \pi)} \simeq \frac{\sigma(e^+ e^- \rightarrow X \rightarrow \Lambda_c \bar{\Lambda}_c)}{\sigma(e^+ e^- \rightarrow X \rightarrow \psi' \pi \pi)} \simeq 23, \quad (5)$$

which is in agreement with Ref. [19].

In summary, this paper demonstrates the evidence of a virtual state in $e^+ e^- \rightarrow X(4660) \rightarrow \Lambda_c \bar{\Lambda}_c$ process with significance of 4.2σ . By employing a model with both s channel $X(4660)$ propagator and $\Lambda_c \bar{\Lambda}_c$ FSI, the data from Belle and BESIII of $e^+ e^- \rightarrow X(4660) \rightarrow (\Lambda_c \bar{\Lambda}_c)$ can be fitted well simultaneously. The virtual state plays a crucial role in respect to that fit since it gives a significant threshold enhancement. This pole is regarded as a $\Lambda_c \bar{\Lambda}_c$ molecular virtual

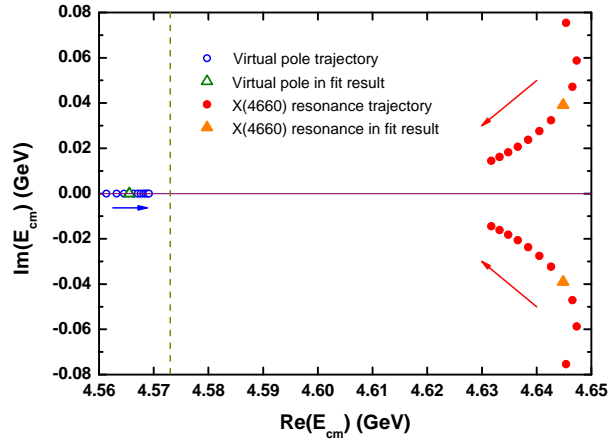


Figure 5: The trajectory of the poles in $W \equiv \sqrt{s}$ plane against the increase of $|\lambda|$. The $|\lambda|$ value increases from 10 GeV^{-2} to 30 GeV^{-2} with the step $\Delta\lambda = 2 \text{ GeV}^{-2}$. The vertical dashed line labels the location of $\Lambda_c \bar{\Lambda}_c$ threshold.

state and would become a bound state if the $\Lambda_c \bar{\Lambda}_c$ contact coupling were larger, while $X(4660)$ is of confinement nature. Finally, since the statistics of the data is limited, the confirmation of it urgently recalls more experimental measurements with higher precisions, such as Belle II, BESIII, LHCb, etc.

Acknowledgments. We would like to thank Guang-Yi Tang for helpful discussions and advices. This work is supported in part by National Nature Science Foundations of China (NSFC) under Contract Nos. 10925522, 11021092.

References

- [1] S. K. Choi *et al.* (Belle Collaboration), Phys. Rev. Lett. **91**, 262001 (2003).
- [2] S. Godfrey and N. Isgur, Phys. Rev. D **32**, 189 (1985).
- [3] M. A. Sultan, N. Akbar, B. Masud, and F. Akram, Phys. Rev. D **90**, 054001 (2014).
- [4] T. Barnes, S. Godfrey, and E. S. Swanson, Phys. Rev. D **72**, 054026 (2005).
- [5] S. F. Radford and W. W. Repko, Phys. Rev. D **75**, 074031 (2007).
- [6] A. P. Szczepaniak, Phys. Lett. B **747**, 410 (2015).
- [7] F. K. Guo, C. Hanhart, Ulf-G. Meißner, Q. Wang, Q. Zhao, and B. S. Zou, Rev. Mod. Phys. **90**, 015004 (2018).
- [8] Z. G. Xiao and Z. Y. Zhou, Phys. Rev. D **94**, 076006 (2016).
- [9] Z. G. Xiao and Z. Y. Zhou, J. Math. Phys. **58**, 062110 (2017).
- [10] Z. G. Xiao and Z. Y. Zhou, J. Math. Phys. **58**, 072102 (2017).
- [11] X. L. Wang *et al.* (Belle Collaboration), Phys. Rev. Lett. **99**, 142002 (2007).
- [12] J. P. Lees *et al.* (BaBar Collaboration), Phys. Rev. D **89**, 111103 (2014).
- [13] X. L. Wang *et al.* (Belle Collaboration), Phys. Rev. D **91**, 112007 (2015).

- [14] G. Pakhlova *et al.* (Belle Collaboration), *Proceedings, 34th International Conference on High Energy Physics (ICHEP2008): Philadelphia, Pennsylvania, July 30-August 5, 2008*, Phys. Rev. Lett. **101**, 172001 (2008).
- [15] L. Y. Dai, J. Haidenbauer, and Ulf-G. Meißner, Phys. Rev. D **96**, 116001 (2017).
- [16] M. Tanabashi *et al.* (Particle Data Group), Phys. Rev. D **98**, 030001 (2018).
- [17] F. K. Guo, J. Haidenbauer, C. Hanhart, and Ulf-G. Meißner, Phys. Rev. D **82**, 094008 (2010).
- [18] B. Q. Li and K. T. Chao, Phys. Rev. D **79**, 094004 (2009).
- [19] G. Cotugno, R. Faccini, A. D. Polosa, and C. Sabelli, Phys. Rev. Lett. **104**, 132005 (2010).
- [20] X. D. Guo, D. Y. Chen, H. W. Ke, X. Liu, and X. Q. Li, Phys. Rev. D **93**, 054009 (2016).
- [21] X. W. Liu, H. W. Ke, X. Liu, and X. Q. Li, Eur. Phys. J. C **76**, 549 (2016).
- [22] L. C. Gui, L. S. Lu, Q. F. Lü, X. H. Zhong, and Q. Zhao, Phys. Rev. D **98**, 016010 (2018).
- [23] M. Ablikim *et al.* (BESIII Collaboration), Phys. Rev. Lett. **120**, 132001 (2018).
- [24] R. B. Ferroli, “*Some anomalies in Baryon Time-like Form Factors*”, a conference talk in “*668. WE-Heraeus-Seminar on Baryon Form Factors: Where do we stand?*”, April 23-27, 2018.
- [25] R. Machleidt, K. Holinde, and C. Elster, Phys. Rept. **149**, 1 (1987).
- [26] Q. R. Gong, Z. H. Guo, C. Meng, G. Y. Tang, Y. F. Wang, and H. Q. Zheng, Phys. Rev. D **94**, 114019 (2016).
- [27] M. Ablikim *et al.* (BESIII Collaboration), Phys. Rev. D **96**, 032004 (2017).
- [28] D. Morgan, Nucl. Phys. A **543**, 632 (1992).
- [29] O. Zhang, C. Meng, and H. Q. Zheng, Phys. Lett. B **680** (2009) 453.
- [30] L. Y. Dai, M. Shi, G. Y. Tang, and H. Q. Zheng, Phys. Rev. D **92**, 014020 (2015).
- [31] Q. R. Gong, J. L. Pang, Y. F. Wang, and H. Q. Zheng, Eur. Phys. J. C **78**, 276 (2018).